11-2012

Gene Duplication and the Evolution of Hemoglobin Isoform Differentiation in Birds

Michael T. Grispo
University of Nebraska-Lincoln, mgrispo@gmail.com

Chandrasekhar Natarajan
University of Nebraska-Lincoln, chandrasekhar.natarajan@unl.edu

Joana Projecto-Garcia
University of Nebraska–Lincoln

Hideaki Moriyama
University of Nebraska-Lincoln, hmoriyama2@unl.edu

Roy E. Weber
Aarhus University, Denmark

See next page for additional authors

Published in *Journal of Biological Chemistry* 287:45 (November 2, 2012), pp. 37647-37658; doi: 10.1074/jbc.M112.375600

Submitted April 24, 2012; revised September 6, 2012; published online September 8, 2012.

This work was supported by National Institutes of Health Grants R01 HL087216 and HL087216-S1 from NHLBI, and also by National Science Foundation Grant IOS-0949931 and the Science Faculty, Aarhus University.

The nucleotide sequences reported in this paper have been submitted to the GenBank™/EBI Data Bank with accession number(s) JQ405307–JQ405317, JQ405319–JQ405326, JQ697045–JQ 97070, JQ405317, and JQ824132.

Supplemental Tables S1 and S2 and additional references are presented following the References.

Gene Duplication and the Evolution of Hemoglobin Isoform Differentiation in Birds

Michael T. Grispo,[1] Chandrasekhar Natarajan,[1] Joana Projecto-Garcia,[1] Hideaki Moriyama,[1] Roy E. Weber,[2] and Jay F. Storz[1]

1. School of Biological Sciences, University of Nebraska–Lincoln, Lincoln, Nebraska 68588, USA
2. Zoophysiology, Institute for Bioscience, Aarhus University, DK-8000 Aarhus C, Denmark
Corresponding author — J. F. Storz, tel 402 472-1114, fax 402 472-2083, email jstorz2@unl.edu

Background: The functional significance of hemoglobin heterogeneity remains a mystery.
Results: In adult birds, the HbD isoform (related to embryonic hemoglobin) exhibits distinct oxygenation properties relative to the major HbA isoform.
Conclusion: Substitutions that distinguish HbD from HbA are not shared with embryonic hemoglobin.
Significance: Differences between isoforms stem from derived (nonancestral) changes in duplicated genes, not from the retention of an ancestral condition.

Abstract. The majority of bird species co-express two functionally distinct hemoglobin (Hb) isoforms in definitive erythrocytes as follows: HbA (the major adult Hb isoform, with α-chain subunits encoded by the α^A-globin gene) and HbD (the minor adult Hb isoform, with α-chain subunits encoded by the α^D-globin gene). The α^D-globin gene originated via tandem duplication of an embryonic α-like globin gene in the stem lineage of tetrapod vertebrates, which suggests the possibility that functional differentiation between the HbA and HbD isoforms may be attributable to a retained ancestral character state in HbD that harkens back to a primordial, embryonic function. To investigate this possibility, we conducted a combined analysis of protein biochemistry and sequence evolution to characterize the structural and functional basis of Hb isoform differentiation in birds. Functional experiments involving purified HbA and HbD isoforms from 11 different bird species revealed that HbD is characterized by a consistently higher O_2 affinity in the presence of allosteric effectors such as organic phosphates and Cl^- ions. In the case of both HbA and HbD, analyses of oxygenation properties under the two-state Monod-Wyman-Changeux allosteric model revealed that the pH dependence of Hb-O_2 affinity stems primarily from changes in the O_2 association constant of deoxy (T-state)-Hb. Ancestral sequence reconstructions revealed that the amino acid substitutions that distinguish the adult-expressed Hb isoforms are not attributable to the retention of an ancestral (pre-duplication) character state in the α^D-globin gene that is shared with the embryonic α-like globin gene.

Keywords. evolution, hemoglobin, molecular evolution, oxygen transport, protein evolution, avian genome, gene family evolution, globin gene family

Abbreviations. isoHb = Hb isoforms; IHP = inositol hexaphosphate; CBD = constant-but-different; RACE = rapid amplification of cDNA end

Hemoglobin (Hb) is one of the most extensively studied proteins in terms of structure-function relationships, and comparative studies of Hbs from non-human animals have made important contributions to this knowledge base (1–4). Despite this detailed understanding, a number of vexing questions about Hb function continue to challenge comparative biochemists and physiologists. One such question concerns the functional and adaptive significance of co-expressing multiple, structurally distinct Hb isoforms (isoHbs) (2, 5–9). Most vertebrate species express functionally distinct isoHbs during different stages of pre-natal development, and in many groups it is also common to co-express different isoHbs during post-natal life. The majority of birds and nonavian reptiles co-express two functionally distinct isoHbs in definitive erythrocytes as follows: HbA (the major adult isoHb, with α-chain subunits encoded by the α^A-globin gene) and HbD (the minor adult isoHb, with α-chains encoded by the α^D-globin gene). HbD typically accounts for ~10–30% of total Hb in definitive erythrocytes, and available evidence indicates that it is generally characterized by an elevated O_2 affinity relative to HbA (10–20).

Insights into the physiological division of labor between the HbA and HbD isoforms may help to explain why the duplicated α^A- and α^D-globin genes have been retained and why the adult expression of α^D-globin has persisted in the majority of avian lineages. Because the HbA and HbD isoforms exhibit consistent differences in O_2-binding properties, regulatory changes in intra-erythrocytic isoHb stoichiometry could provide a mechanism for modulating blood-O_2 affinity in response to changes in O_2 availability or changes in internal metabolic demand (11, 20, 21).

Another distinction between the two avian isoHbs is that tetrameric HbDs self-associate upon deoxygenation, which results in super-cooperativity (Hill coefficients >4.0) because higher order allosteric interactions between HbD tetramers are

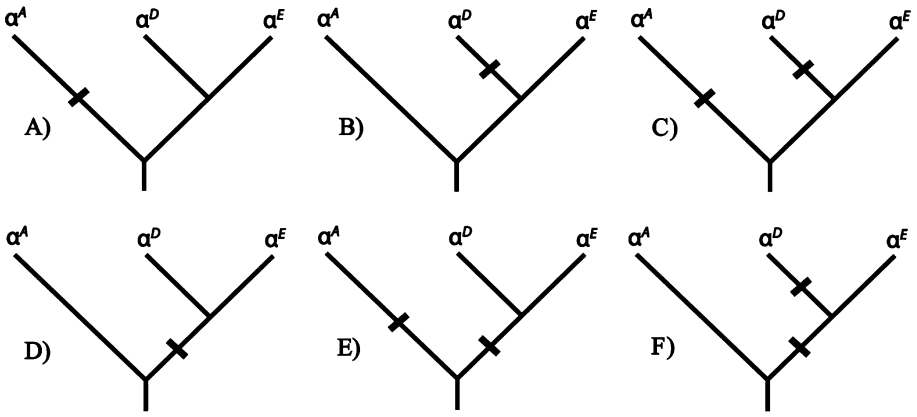

Figure 1. Hypothetical scenarios depicting the phylogenetic distribution of amino acid substitutions that are responsible for functional differentiation between the co-expressed HbA and HbD isoforms in birds. The phylogeny represented in each panel depicts the known branching relationships among the α^A-, α^D-, and α^E-globin genes. At any given site, fixed differences between the α^A- and α^D-globin genes could be attributable to a substitution that occurred on the branch leading to α^A-globin (*A*), a substitution that occurred on the post-duplication branch leading to α^D-globin (*B*), substitutions that occurred on the branch leading to α^A-globin and on the post-duplication branch leading to α^D-globin (*C*), a substitution that occurred on the pre-duplication branch leading to the single-copy progenitor of α^D- and α^E-globin (*D*), substitutions that occurred on the branch leading to α^A-globin and on the pre-duplication branch leading to the α^D/α^E ancestor (*E*), or substitutions that occurred on the pre-duplication branch leading to the α^D/α^E ancestor and on the post-duplication branch leading to α^D-globin (*F*).

superimposed on the subunit-subunit interaction within tetramers (16, 22–24). In principle, the enhanced cooperativity could facilitate efficient O_2 unloading over an especially narrow range of blood O_2 tensions (25).

It is also possible that the physiological benefits of Hb heterogeneity are unrelated to O_2-binding properties. If isoHbs with different isoelectric points co-occur in the same erythrocytes, then Hb heterogeneity may enhance solubility (and hence, corpuscular Hb concentration), thereby increasing the O_2-carrying capacity of the blood (26–28). isoHbs with different charges would also indirectly influence the distribution of protons and other ions across the red cell membrane by altering the Donnan equilibrium, and this could play an important role in the allosteric regulation of Hb-O_2 affinity and cellular metabolism (29, 30). These considerations led Ingermann (8) to conclude that it "… seems unlikely that the presence of electrophoretically distinguishable Hb multiplicity represents selectively neutral variations in Hb structure and function."

Available evidence suggests that the tetrapod common ancestor possessed three tandemly linked gene duplicates that encode the α-chain subunits of the $\alpha_2\beta_2$ Hb tetramer, 5′-α^E–α^D–α^A-3′ (31–33). In the stem lineage of tetrapods, the proto-α^E- and α^A-globin genes originated via tandem duplication of an ancestral α-like globin gene, and α^D-globin originated subsequently via tandem duplication of the proto-α^E-globin gene (31). In tetrapod vertebrates, the α^E-globin gene is exclusively expressed in larval/embryonic erythroid cells, and the α^A-globin gene is expressed in definitive erythroid cells during later stages of prenatal development and postnatal life. In birds and nonavian reptiles that have been studied to date, the α^D-globin gene is expressed in both primitive and definitive erythroid cells (34–36). HbD does not appear to be expressed in the definitive erythrocytes of crocodilians (37–39), and the α^D-globin gene has been inactivated or deleted independently in amphibians and mammals (31, 40, 41).

Given that HbA and HbD share the same β-chain subunits, functional differences between the two isoHbs must be attributable to amino acid substitutions in the α^A- and/or α^D-globin genes. In light of what is known about the phylogenetic history of the α-like globin genes in tetrapods (31, 32), functional differentiation between the HbA and HbD isoforms may be attributable to post-duplication substitutions that occurred in the α^A-globin and/or α^D-globin gene lineages (Figure 1, *A–C*), they could be attributable to substitutions that occurred in the single copy, pre-duplication ancestor of the α^E- and α^D-globin genes (Figure 1*D*), or they could be attributable to a combination of pre- and post-duplication substitutions (Figure 1, *E* and *F*). Because embryonic and adult-expressed Hbs exhibit a number of consistent functional differences (42), the scenarios depicted in Figure 1, *D–F,* suggest the possibility that HbA/D isoform differentiation may be attributable to a retained ancestral character state in HbD that harkens back to a primordial, embryonic function. To investigate this possibility and to examine the functional evolution of the α-like globin genes, we conducted a combined analysis of protein biochemistry and sequence evolution to characterize the structural and functional basis of Hb isoform differentiation in birds. The main objectives were as follows: (i) to characterize the O_2-binding properties of HbA and HbD in species that are representative of several major avian lineages; (ii) to gain insight into the structural basis of the observed functional differentiation between the HbA and HbD isoforms; and (iii) to determine whether functional differentiation between the HbA and HbD isoforms is primarily attributable to post-duplication substitutions or the retention of ancestral character states shared by HbD and embryonic Hb. Functional experiments involving purified HbA and HbD isoforms from 11 different bird species confirmed that HbD is characterized by a consistently higher O_2 affinity in the presence of allosteric effectors such as organic phosphates and Cl^- ions. Results of the comparative sequence analysis revealed that isoHb differentiation is attributable to roughly equal numbers of post-duplication amino acid substitutions that occurred in the α^A- and α^D-globin genes.

Experimental Procedures

Experimental Measures of Hemoglobin Function. To characterize the nature of isoHb differentiation in birds, we

measured O_2-binding properties of purified HbA and HbD isoforms from a total of 11 avian species representing each of six orders as follows: griffon vulture, *Gyps fulvus* (Accipitriformes, Accipitridae); greylag goose, *Anser anser* (Anseriformes, Anatidae); amazilia hummingbird, *Amazilia amazilia* (Apodiformes, Trochilidae); green-and-white hummingbird, *Amazilia viridicauda* (Apodiformes, Trochilidae); violet-throated starfrontlet, *Coeligena violifer* (Apodiformes, Trochilidae); giant hummingbird, *Patagona gigas* (Apodiformes, Trochilidae); great-billed hermit, *Phaethornis malaris* (Apodiformes, Trochilidae); common pheasant, *Phasianus colchicus* (Galliformes, Phasianidae); rook, *Corvus frugilegus* (Passeriformes, Corvidae); house wren, *Troglodytes aedon* (Passeriformes, Troglodytidae); and ostrich, *Struthio camelus* (Struthioformes:, Struthionidae). We examined Hbs from a disproportionate number of hummingbirds because Apodiformes is the most speciose order of birds after the passerines, and because this group is under-represented in previously published studies of avian Hb function.

Blood samples were obtained according to methods described by Weber *et al.* (20) and Nothum *et al.* (14). Washed red cells were frozen at −70 °C and were subsequently thawed by adding 2 volumes of distilled water and □ volume of 1 m Tris/HCl buffer, pH 7.5. For each individual specimen, Hb isoform composition was characterized by means of alkaline PAGE and/or thin layer isoelectric focusing (PhastSystem, GE Healthcare Biosciences). Depending on the species, the HbA and HbD isoforms were separated by fast protein liquid chromatography (FPLC), DEAE anion-exchange chromatography, CM-Sepharose cation-exchange chromatography, and/or preparative electrofocusing, as described previously (11, 36, 43, 44). The separate isoHbs were further stripped of organic phosphate and other ions by passing the samples through a mixed bed resin column (MB-1 AG501-X8; Bio-Rad) using FPLC. Hb solutions were then saturated with carbon monoxide and dialyzed at 5 °C for at least 24 h against three changes of CO-saturated 0.01 m Tris/HCl buffer, pH 7.5, containing 0.5 mm EDTA. In cases where partial oxidation (metHb formation) was evident, Hb was reduced by adding sodium dithionite, followed by dialysis against Tris buffer containing EDTA, as described by Weber *et al.* (20). For the Hbs of the house wrens and the five hummingbird species, we used 10 mm HEPES as the dialysis buffer.

We measured O_2 equilibrium curves for purified HbA and HbD isoforms using a modified gas diffusion chamber coupled to cascaded Wösthoff pumps for mixing pure N_2 (99.998%), O_2, and atmospheric air (9). Changes in the absorbance spectra of thin layer Hb solutions (4 μl) were measured in conjunction with stepwise changes in the partial pressure of O_2 (PO_2) inside the chamber. Values of P_{50} (the PO_2 at which heme is 50% saturated) and n_{50} (Hill's cooperativity coefficient at 50% saturation) were interpolated from linear plots of $\log(Y/(Y-1))$ *versus* $\log PO_2$ for at least four values of Y (fractional saturation) between 0.25 and 0.75. To assess variation in the sensitivity of Hb-O_2 affinity to allosteric effectors (ligands that alter Hb-O_2 affinity by reversibly binding to sites remote from the active site), we measured O_2 equilibrium curves of Hbs suspended in 0.10 m NaHEPES buffer, in the absence of added effectors ("stripped"), in the presence of inositol hexaphosphate (IHP (IHP/Hb tetramer ratio = 2.0)), in the presence of 0.10 m Cl^- ions (added as potassium chloride, KCl), and in the presence of both effectors ([heme], 0.3 mm, unless otherwise specified). IHP is a chemical analog of inositol pentaphosphate, which is the most potent allosteric effector molecule in avian red cells (21, 45).

In the case of pheasant HbA and HbD, we conducted a detailed analysis of allosteric interactions based on measurements of O_2 equilibria that included extremely high and extremely low saturation values. This allowed us to analyze the data in terms of the two-state Monod-Wyman-Changeux allosteric model (46), which relates Hb-O_2 saturation (Y) to the partial pressure of O_2 (P), the O_2 association constants for "R-state" oxyHb and "T-state" deoxy-Hb (K_R and K_T, respectively), the allosteric constant (L), and the number of interacting O_2-binding sites (q) as shown in Equation 1.

$$Y = \frac{LK_TP\{1 + K_TP\}^{(q-1)} + K_RP\{1 + K_RP\}^{(q-1)}}{L(1 + K_TP)^q + (1 + K_RP)^q} \quad (1)$$

This equation was fit to the data in the form $\log(Y/1-Y)$ *versus* $\log P$ (end-weighting), and parameters were estimated using the curve-fitting procedure described by Weber *et al.* (47). In separate analyses, values of q were estimated from the data or were fixed at 4, as applies to tetrameric Hb. The two-state Monod-Wyman-Changeux parameters derived for $q = 4$ were used to calculate the intrinsic Adair constants that characterize the affinities of four successive heme oxygenation steps (48, 49) as shown in Equation 2.

$$\begin{aligned} k_1 &= (K_R + LK_T) / (1 + L) \\ k_2 &= (K_R^2 + LK_T^2) / (K_R + LK_T) \\ k_3 &= (K_R^3 + LK_T^3) / (K_R^2 + LK_T^2) \\ k_4 &= (K_R^4 + LK_T^4) / (K_R^3 + LK_T^3) \end{aligned} \quad (2)$$

The half-saturation value, P_{50}, was calculated as the PO_2 at $\log[Y/(1-Y)] = 0$, and the median PO_2, P_m, was calculated as shown in Equation 3,

$$P_m = \left\{\frac{1}{K_R}\right\}\left(\frac{L+1}{Lc^q+1}\right)^{1/q} \quad (3)$$

where $c = K_T/K_R$ (50). The maximum slope of the log-log plot, n_{max}, was calculated by first solving for PO_2 in Equation 4,

$$\frac{d^2\left\{\log\left(\frac{s}{1-s}\right)\right\}}{d\{\log(PO_2)\}^2} = 0 \quad (4)$$

and then using that value to calculate $d(\log[Y/(1-Y)]/d(\log PO_2)$. The free energy of cooperativity, ΔG, was calculated as in Equation 5.

$$\Delta G = \frac{RT\ln\{(L+1)(Lc^q+1)\}}{(Lc+1)(Lc^{q-1}+1)} \quad (5)$$

Our O_2 binding data are not strictly comparable with those of some previously published studies because some workers measured O_2 equilibria using ionic buffers that change Hb-O_2

affinity via pH-dependent perturbations in the free concentration of allosteric effectors (51). Nonetheless, measurements of O_2-binding properties for HbA and HbD should be internally consistent within a given study, so it is possible to compare relative levels of isoHb differentiation among studies. Thus, for the purpose of making broad scale comparisons of isoHb differentiation among species, we surveyed published studies of avian Hbs and compiled measures of the difference in log-transformed P_{50} values between HbA and HbD in the presence and absence of IHP.

Molecular Modeling. We built homology-based structural models of pheasant HbA and HbD isoforms using SWISS-MODEL (52). We used deoxyhemoglobin (Protein Data Bank ID, 2HHB) as a template to maintain consistency with the results of Riccio *et al.* (53) and Tamburrini *et al.* (18). The root mean square deviations between the templates and models of the α^A-, α^D-, and β-chains were less than 0.08, 0.09, and 0.10 Å, respectively. These structures were used to calculate surface potentials using the PBEQ solver found on the CHARMM GUI server (54). We used the Swiss Institute of Bioinformatics ExPASy proteomics server (55) to estimate the isoelectric point (pI) of the observed and reconstructed α-chain globin structures. Finally, we conducted molecular dynamics simulations to predict O_2 and IHP binding energies using AutoDock Vina (56). The search box for IHP (3HXN) was 25 Å cubic centered on the α-chain dyad cleft and that for O_2 (1DN2) was 5 Å cubic centered on the O_2-binding heme iron.

Taxon Sampling for the Molecular Evolution Analysis. Our phylogenetic survey of amino acid divergence among the avian α-like globin genes included a total of 54 species, including 10 of the 11 species that were used as subjects for the experimental studies of Hb function (supplemental Table S1). We cloned and sequenced the α^A-, α^D-, and/or α^E-globin genes from 28 of the bird species, and we retrieved the remaining sequences from public databases. We also included 98 homologous α-like globin sequences from species that are representative of the other main tetrapod lineages (amphibians, nonavian reptiles, and mammals) as well as teleost fish (supplemental Table S2).

Molecular Cloning and Sequencing. Genomic DNA was isolated from frozen liver tissues using the DNeasy kit, and RNA was isolated from frozen whole blood or frozen pectoral muscle using the RNeasy kit (Qiagen, Valencia, CA). We designed paralog-specific PCR primer combinations for the α^E-, α^D-, and α^A-globin genes by using multispecies alignments of orthologous sequences that have been annotated in avian genome assemblies (32, 41, 57). For each species, the α^E-globin gene was PCR-amplified from genomic DNA using the Invitrogen Taq polymerase native kit (Invitrogen) and the following thermal cycling protocol: 94 °C (10 min) initial denaturing (94 °C (30 s), 54–62.5 °C (30 s), and 72 °C (1 min)) for 34 cycles, followed by a final extension at 72 °C (7 min). The α^D- and α^A-globin genes were PCR-amplified from genomic DNA, as described above, or cDNAs were amplified from RNA using the Qiagen OneStep RT-PCR kit (Qiagen, Valencia, CA). Reverse transcriptase (RT)-PCRs were conducted according to the following thermal cycling protocol: 50 °C (30 min) followed by a 94 °C (15 min) initial denaturing, (94 °C (30 s), 55 °C (30 s), 72 °C (1 min)) for 34 cycles, followed by a final extension at 72 °C (3 min).

For some species, we sequenced the α^A- and α^D-globin coding regions by using rapid amplification of cDNA ends (RACE). Primers were designed in the conserved exonic regions of the α^A- and α^D-globin genes, and the first strand synthesis was carried out using SuperScript™ II reverse transcriptase (Invitrogen). Both 5′- and 3′-RACE were performed according to the manufacturer's protocol. Sequences of all PCR, RT-PCR, and RACE primers are available upon request.

PCR products were electrophoretically separated on a 1.2% agarose gel (100 volts) and were then excised and eluted from the gel following the protocol in the QIAquick gel extraction kit (Qiagen, Valencia, CA). PCR amplicons were cloned into pCR4-TOPO vector (Invitrogen), which was then used to transfect One-shot TOP10 chemically competent *Escherichia coli* cells (Invitrogen). Positive clones were sequenced on an ABI 3730XL high throughput capillary DNA analyzer (Applied Biosystems, Foster City, CA) using internal T7/T3 primers. All sequences were deposited in GenBank™ under the accession numbers: JQ405307–JQ405317, JQ405319–JQ405326, JQ697045–JQ697070, JQ405318, and JQ824132.

Prediction of Functionally Divergent Sites. To nominate candidate sites for functional divergence between the avian α^A- and α^D-globin sequences, we identified residue positions that were highly conserved within each paralogous clade but differed between the two clades. Such sites were termed "constant-but-different" (CBD) sites by Gribaldo *et al.* (58) and were termed "type II" divergent sites by Gu (59). Our analysis of functional divergence was based on a total of 92 sequences (47 avian α^A-globin sequences and 45 avian α^D-globin sequences). To quantify the conservation of physicochemical properties at each residue position within the separate sets of α^A- and α^D-globin sequences, we calculated site-specific entropy values (60) as shown in Equation 6,

$$H_j = -\sum_j^i p_j \log_b p_j \quad (6)$$

where p_j is the frequency of a particular physicochemical state at site j, and $b = 8$ such that calculated values fall within the interval (0, 1). In addition to considering single-residue insertions or deletions, we considered eight possible physicochemical states for each residue position as follows: hydrophobic (Ala, Val, Ile, and Leu), hydrophilic (Ser, Thr, Asn, and Gln), sulfur-containing (Met and Cys), glycine (Gly), proline (Pro), acidic (Asp and Glu), basic (His, Lys, and Arg), and aromatic (Phe, Trp, and Tyr). We identified CBD sites as residue positions that were highly conserved within each set of orthologous sequences (H_i <0.5) but exhibited a consistent physicochemical difference between the α^A- and α^D-globin sequences. CBD sites do not necessarily represent fixed amino acid differences between the α^A- and α^D-globin paralogs, because a given site could be variable for an interchangeable set of isomorphous residues within each set of orthologous sequences.

Ancestral Sequence Reconstruction. To infer the phylogenetic distribution of amino acid substitutions that contributed to functional differentiation between the avian HbA and HbD isoforms, we reconstructed ancestral sequences at

four separate nodes in the phylogeny of α-like globin genes as follows: (i) the single-copy proto-α-globin gene in the stem lineage of tetrapod vertebrates; (ii) the ancestral α^A-globin in the stem lineage of birds; (iii) the single-copy ancestor of the α^E- and α^D-globin paralogs in the stem lineage of tetrapods; and (iv) the ancestral α^D-globin in the stem lineage of birds. To reconstruct ancestral α-chain sequences, we applied the maximum likelihood approach of Yang *et al.* (61) using the WAG + F model of amino acid substitution (62, 63) as implemented in PAML 4.4 (64). Amino acid sequences were aligned using the default parameters in Muscle (65). The ancestral sequence reconstruction was based on a phylogeny of α-like globin sequences from a representative set of mammals, birds, nonavian reptiles, and amphibians, and the tree was rooted with α-globin sequences from teleost fishes. Ancestral states of individual sites were reconstructed independently, and we restricted the analysis to sites that had posterior probabilities ≥0.8 for a given residue or physicochemical property.

In the phylogeny of α-like globin genes, (α^A (α^D and α^E)), site-specific amino acid differences between the avian α^A- and α^D-globin sequences could be attributable to substitutions on (i) the branch leading to α^A, (ii) the post-duplication branch leading to α^D, and/or (iii) the pre-duplication branch leading to the single copy ancestor of α^D and α^E (Figure 1). Accordingly, we identified all amino acid substitutions that distinguish the avian α^A- and α^D-globin paralogs, and after reconstructing ancestral states at relevant nodes of the phylogeny, we mapped the observed substitutions onto the branches mentioned above. Mapping charge-changing substitutions onto branches of the phylogeny also allowed us to reconstruct the causes of divergence in isoelectric point (pI) between the HbA and HbD isoforms.

Results

Relative Abundance of HbA and HbD. Ten of the bird species included in our study expressed two main Hb isoforms that were clearly referable to HbA and HbD. The griffon vulture, *G. fulvus*, expressed three isoHbs, one of which is clearly identifiable as HbD, and the other two incorporated the products of duplicated α^A-globin genes (HbA and HbA′). The species that we examined generally expressed the HbA and HbD isoforms in a 2:1–4:1 ratio, which is consistent with results from previous studies (8). The pheasant represented the sole exception to this pattern, as HbD was present at a higher concentration than HbA (69 *versus* 31%). HbD expression has been secondarily lost in representatives of six avian orders (Ciconiiformes, Columbiformes, Coraciformes, Cuculiformes, Psittaciformes, and Sphenisciformes), and parsimony-based character-state mapping (using the phylogeny of Hackett *et al.* (66)) suggests that each of these losses occurred independently (data not shown).

Functional Properties of Avian HbA and HbD Isoforms. O_2-equilibrium measurements revealed consistent functional differences between the HbA and HbD isoforms, as HbD was generally characterized by a higher O_2 affinity (lower P_{50}) in the presence of IHP (2-fold molar excess over Hb) and in the presence of IHP + 0.1 m Cl^- (Table 1). This pattern of isoHb differentiation is consistent with previously published results for avian Hbs (Table 2). HbD was generally characterized by a higher intrinsic O_2 affinity than HbA, but there were several exceptions. In the griffon vulture, HbD showed a much lower O_2 affinity than HbA in the absence of effectors but a higher affinity in the presence of IHP (Table 1). Likewise, in 4 of the 5 hummingbird species that we examined (amazilia hummingbird, green-and-white hummingbird, violet-throated starfrontlet, and great-billed hermit), the HbA isoform exhibited a slightly higher intrinsic O_2 affinity than HbD. In all cases these differences in O_2 affinity were reversed in the presence of IHP (Table 2). Vandecasserie *et al.* (19) also reported that the HbA isoforms of mallard duck, pheasant, and turkey had higher intrinsic O_2 affinities than the co-expressed HbD isoforms, and again, this was reversed in the presence of anionic effectors (Table 2). Contrary to the results reported by Vandecasserie *et al.* (19), our O_2-equilibrium measurements on pheasant Hbs revealed a lower O_2 affinity in HbA than in co-expressed HbD in the presence *and* in the absence of anionic effectors, as found in most other species that express both isoforms (Tables 1 and 2). Whereas our O_2-binding experiments were carried out using zwitterionic HEPES buffer, those by Vandecasserie *et al.* (19) were carried out using an ionic Tris/HCl buffer that may perturb the measurements of O_2 affinity by reducing the concentration of free anionic effectors in a pH-dependent manner (51). Our results and those of Vandecasserie *et al.* (19) are in agreement that the O_2 affinity of HbA is lower than that of HbD in the presence of anionic effectors, the state that is most relevant to *in vivo* conditions.

The O_2 affinities of pheasant HbA and HbD were modulated by pH in a similar fashion, as estimated Bohr factors were virtually identical for both isoHbs ($\varphi = \Delta\log P_{50}/\Delta pH = -0.43$ at 25 °C and pH 7.0–7.5). The Bohr factor was slightly reduced at 37 °C (φ for HbA = −0.37), in accordance with the temperature dependence of proton dissociation, but it was strongly increased in the presence IHP ($\varphi = -0.63$ at 37 °C), which is consistent with the induction of basic proton binding groups by this anionic effector (67). When stripped of allosteric effectors, HbA and HbD exhibited similar cooperativity coefficients ($n_{50} \sim 2.0$ at 37 °C and pH 7.0–7.5) that increased in the presence of IHP ($n_{50} \sim 2.6$). The mixture of purified HbA and HbD isoforms exhibited P_{50} values that were intermediate to those of the individual isoHbs at physiological pH (Figure 2), which indicates the absence of functionally significant intracellular interaction between the two isoforms, as observed previously for chicken Hb at high Hb concentration (16). This lack of interaction, in conjunction with the observed symmetry of O_2-binding curves (reflected by the correspondence between n_{max} and n_{50} values and between P_m and P_{50} values; Table 3), justifies the quantification of the allosteric interactions of both isoforms in terms of shifts in P_{50} values (68).

Extended Hill plots for the HbA and HbD isoforms (Figure 3) and estimates of the Monod-Wyman-Changeux parameters (Table 3) elucidate the allosteric control mechanisms that underlie the observed hetero- and homotropic effects. When measured at the same pH, extended Hill plots for HbA and HbD are almost superimposed, revealing nearly identical association constants in the deoxygenated and oxygenated states (K_T and K_R, which can be interpolated from the intercepts of the lower and the upper asymptotes, respectively, of the extended Hill plots with the vertical line at log $PO_2 = 0$; Figure

Table 1. O_2 affinities (P_{50}, torr) and cooperativity coefficients (n_{50}) of purified HbA and HbD isoforms from 11 bird species. O_2 equilibria were measured in 0.1 mm HEPES buffer at pH 7.4 (± 0.01) and 37 °C in the absence (stripped) and presence of allosteric effectors ([Cl^-], 0.1 m; [HEPES], 0.1 m; IHP/Hb tetramer ratio, 2.0. P_{50} and n_{50} values were derived from single O_2 equilibrium curves, where each value was interpolated from linear Hill plots (correlation coefficient r> 0.995) based on four or more equilibrium steps between 25 and 75% saturation.

			Stripped		+ KCl		+ IHP		+ KCl + IHP	
Species	IsoHb	[Heme], mm	P_{50}	N_{50}	P_{50}	n_{50}	P_{50}	n_{50}	P_{50}	n_{50}
Accipitriformes										
Gyps fulvus	HbA	0.30			6.46	1.62			28.84	1.98
	HbD	0.07			15.86	1.82			26.61	1.99
Anseriformes										
Anser anser	HbA	1.00			4.78	2.51			43.95[a]	3.00[a]
	HbD	0.72			3.59	1.90			29.79[a]	2.51[a]
Apodiformes										
A. amazilia	HbA	0.30	3.14	1.38	5.28	1.90	36.77	2.16	29.84	2.42
	HbD	0.30	3.36	1.70	4.79	2.08	28.61	2.63	23.20	2.40
A. viridicauda	HbA	0.30	2.62	1.43	4.47	1.81	28.49	2.13	24.24	2.07
	HbD	0.30	2.78	1.34	3.90	1.64	21.83	2.22	20.36	2.29
C. violifer	HbA	0.30	2.12	1.29	3.74	1.65	23.55	1.96	19.12	1.70
	HbD	0.30	2.48	1.40	3.65	1.80	17.70	2.30	17.01	2.46
P. gigas	HbA	0.30	2.52	1.46	4.14	1.63	29.97	2.28	25.86	2.49
	HbD	0.30	2.45	1.41	3.19	1.97	17.44	2.24	16.56	2.56
P. malaris	HbA	0.30	2.83	1.39	4.70	1.83	37.00	2.27	28.13	2.04
	HbD	0.30	3.06	1.62	5.02	2.11	26.03	2.47	24.92	2.72
Galliformes										
Phasianus colchicus	HbA	0.08			5.62	1.86			44.67[a]	2.31[a]
	HbD	0.11			5.54	1.73				
	HbA	0.60			4.12[b]	2.47[b]			29.51[b]	2.55[b]
	HbD	0.60			3.50[b]	2.38[b]			24.24[a,b]	2.46[a,b]
Passeriformes										
Corvus frugilegus	HbA	0.06			5.60	1.50				
	HbD	0.04			4.15	1.46				
Troglodytes aedon	HbA	0.30	2.80	1.48	4.57	1.91	33.90	1.98	25.87	2.11
	HbD	0.30	1.58	1.47	2.67	1.92	22.59	2.39	16.28	2.36
Struthioformes										
Struthio camelus	HbA	0.58			3.55	1.90			32.73[a]	2.85
	HbD	0.58			2.63	1.75			22.90[a]	2.44

a. Saturating IHP/Hb4 ratio is >20.
b. These values are taken from Table 3 (Monod-Wyman-Changeux parameters), temperature = 25 °C.

3*A*). Thus, both isoHbs are characterized by similar free energies of Hb cooperativity (ΔG = ~8.4 and ~8.0 for HbA and HbD, respectively, with q = free at pH ~7.5; Table 3). Whereas increased proton activity (decreased pH) reduces O_2 affinity by lowering K_T without markedly affecting K_R, IHP decreases O_2 affinity by lowering K_T more than K_R, such that both effectors raise ΔG. The effect of IHP on both K_T and K_R (Figure 3*B*), indicates that this effector binds to the deoxy as well as the oxy structures. Similar effects of IHP have been documented in human and fish Hbs, although physiological levels of the autochthonous phosphate effectors (2,3-diphosphoglycerate and ATP, respectively) primarily modulate K_T (69, 70). As shown in Figure 3*B*, increased temperature lowers K_R more than K_T, thereby decreasing the free energy of heme-heme cooperativity.

The allosteric T-state → R-state transitions of pheasant HbA and HbD and their dependence on modulating factors are further illustrated by the Adair association constants (k_{1-4}) for the four successive oxygenation steps. In stripped HbA and HbD at pH ~7.5, the similar k_1 and k_2 constants and the markedly increased k_3 and k_4 values indicate that the allosteric transition occurs only after binding the second and third O_2 molecules (Figure 4). This also applies at low pH (~7.0), where lower k_1 and k_2 values show that proton binding reduces the affinities for binding the 1st and 2nd O_2 molecules. In the presence of IHP, the even lower values of k_1, k_2, and k_3 combined with a drastically increased k_4 (Figure 4) indicate that IHP suppresses the affinities of unliganded hemes for the 1st, 2nd, and 3rd O_2 molecules but has little effect on the affinity of the remaining unliganded heme. This indicates that IHP-binding delays the T-state → R-state transition in quaternary structure until the final oxygenation step.

Insights into the Evolutionary Origins of Hb Isoform Differentiation. Comparison of avian α^A and α^D sequences yielded a Poisson-corrected amino acid divergence of 35.6%. We identified a total of 39 candidate sites that may contribute to functional divergence between the avian α^A- and α^D-globin genes (Figure 5), 33 of which are CBD sites (both paralogs having H_i values <0.50; sites 1, 8, 9, 11, 12, 28, 53, 57, 67, 68, 71, 72, 75, 77, 78, 82, 85, 89, 90, 102, 106, 113–117, 124, 125, 130, 133, 134, 137, and 138). The remaining six sites were more variable in one or both sets of orthologous sequences (sites 5, 15, 18, 21, 30, and 50). Ancestral sequence reconstructions revealed that roughly equal numbers of substitutions occurred on the post-duplication branches leading to α^A- and α^D-globin. Substitutions at 11 sites were consistent with the scenario depicted in Figure 1*A*; substitutions at 12 sites were consistent with Figure 1*B*, and substitutions at five sites were consistent with Figure 1*C*. None of the divergent sites between the α^D- and α^A-globin sequences were consistent with the scenarios depicted in Figure 1, *D* and *E* or *F*. The pattern was similar when we considered the complete set of 39 substitutions (including sites for which

Table 2. O_2 affinity differences between avian HbA and HbD isoforms in the absence of allosteric effectors (stripped) and in the presence of IHP. IHP was present at saturating concentrations (IHP/Hb_4 ratio >20), except where indicated.

	$\Delta\log P_{50}$ (HbA - HbD)					
Species	Stripped/+KCl	+IHP	°C	pH	Buffer	Ref.
Accipitriformes						
Gyps fulvus	−0.37[a]	0.06[a]	37	7.4	0.1 m NaHEPES, 0.1 m KCl	This study
	−0.41[b]		37	7.4	0.1 m NaHEPES, 0.1 m KCl	This study
Gyps ruppellii	0.20[a]	~0.40[a]	38	7.5	0.1 m NaHEPES, 0.1 m KCl	Weber *et al.* (20)
	0.09[b]	~0.20[b]	38	7.5	0.1 m NaHEPES, 0.1 m KCl	Weber *et al.* (20)
Trigonoceps occipitalis	0.10	0.06	38	7.5	0.1 m NaHEPES, 0.1 m KCl	Hiebl *et al.* (12)
Anseriformes						
Anas platyrhinchos	−0.32	0.45[c]	20	7.0	0.025 m TrisHCl/0.1 m NaCl	Vandecasserie *et al.* (19)
Anser anser		0.17	37	7.4	0.1 m NaHEPES, 0.1 m KCl	Present study
Apus apus	0.23	0.54	38	7.5	0.02 m TrisHCl/0.1 m NaCl	Nothum *et al.* (14)
Apodiformes						
A. amazilia	−0.03	0.11	37	7.4	0.1 m NaHEPES, 0.1 m KCl	Present study
A. viridicauda	−0.03	0.12	37	7.4	0.1 m NaHEPES, 0.1 m KCl	Present study
C. violifer	−0.07	0.12	37	7.4	0.1 m NaHEPES, 0.1 m KCl	Present study
P. gigas	0.01	0.24	37	7.4	0.1 m NaHEPES, 0.1 m KCl	Present study
P. malaris	−0.03	0.15	37	7.4	0.1 m NaHEPES, 0.1 m KCl	Present study
Charadriiformes						
Catharacta maccormicki	0.20	~0.15	37	7.5	0.1 m NaHepes /0.1 m NaCl	Tamburrini *et al.* (18)
Galliformes						
Gallus gallus	0.14	0.61[c]	20	7.0	0.025 m TrisHCl/0.1 m NaCl	Vandecasserie *et al.* (19)
	0.55	0.88	25	7.0	0.1 m NaHEPES, 0.1 m KCl	Weber *et al.* (44)
Meleagris gallopavo	−0.27	0.35[c]	20	7.0	0.025 m TrisHCl/0.1 m NaCl	Vandecasserie *et al.* (19)
Phasianus colchicus	−0.37	0.20[c]	20	7.0	0.025 m TrisHCl/0.1 m NaCl	Vandecasserie *et al.* (19)
	0.01		37	7.4	0.1 m NaHEPES, 0.1 m KCl	Present study
	0.07	0.09	25	7.5	0.1 m NaHEPES, 0.1 m KCl	Present study
Passeriformes						
Corvus frugilegus	0.13		37	7.4	0.1 m NaHEPES, 0.1 m KCl	Present study
Troglodytes aedon	0.25	0.18	37	7.4	0.1 m NaHEPES, 0.1 m KCl	Present study
Phoenicopteriformes						
Phoenicopterus roseus	0.24	~0.50	20	7.5	0.05 m TrisHCl/0.1 m NaCl	Sanna *et al.* (17)
Struthioniformes						
Struthio camelus	0.30	0.48[c]	37	7.4	0.05 m TrisHCl/0.2 m NaCl	Oberthür *et al.* (15)
	0.13	0.16	37	7.4	0.1 m NaHEPES, 0.1 m KCl	Present study

a. Comparison was between HbA and HbD.
b. Comparison was between HbA′ and HbD.
c. IHP/Hb tetramer ratio is 1:1.

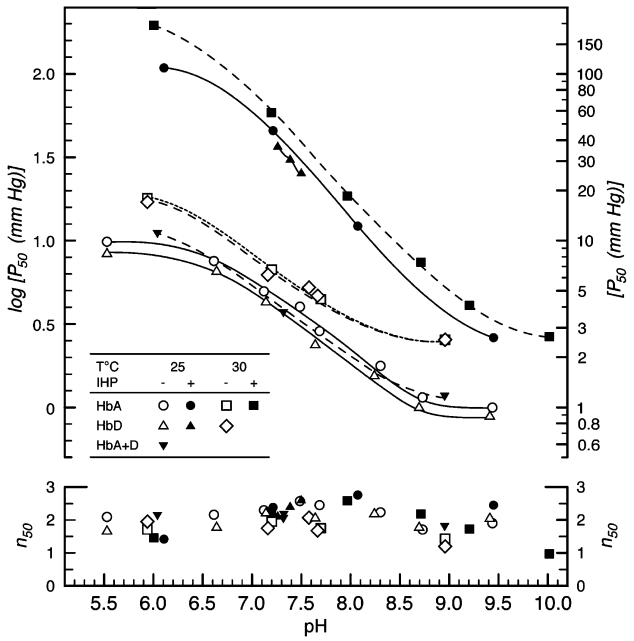

Figure 2. O_2 affinity and cooperativity (P_{50} and n_{50}, respectively) of pheasant HbA and HbD as a function of pH, temperature, and in the absence and presence of IHP (IHP/$H4_B$ ratio = 23.5). O_2 equilibria were measured in 0.1 m NaHEPES buffer containing 0.1 m KCl. Heme concentration, 0.08 mm (HbA) and 0.11 mm (HbD) and 0.10 (HbA +D).

ancestral state reconstructions had posterior probabilities <0.8). The sole exception is that the inferred history of substitution at site α9 was consistent with the scenario depicted in Figure 1*D*.

Charge-changing substitutions at 17 solvent-exposed residue positions account for the observed difference in net surface charge between HbA (mean pI = 8.67) and HbD (mean pI = 7.09). Substitutions at eight sites were consistent with the scenario depicted in Figure 1*A* (71, 89, 90, 116, 117, 130, and 138), substitutions at eight sites were consistent with the scenario depicted in Figure 1*B* (11, 30, 53, 68, 75, 82, 85, and 115), and substitutions at two sites were consistent with the scenario depicted in Figure 1*C* (8 and 15).

Insights into the Structural Basis of Hb Isoform Differentiation. The simulation-based autodocking experiments predicted a slightly lower O_2-binding energy (and hence higher O_2 affinity) for the α-chain heme groups of HbD relative to those of HbA, −0.5 kcal/mol *versus* −0.4 kcal/mol, respectively. The molecular dynamics simulations also predicted that the "additional" α-chain phosphate-binding site of HbD (*sensu* Tamburrini *et al.* (18) and Riccio *et al.* (53)) has a slightly lower IHP-binding energy relative to that of HbA (Table 4) and that the bound IHP molecule is lodged more deeply in the α-chain binding cleft of HbD (Figure 6). This isoform difference in the stereochemistry of IHP binding is mainly attributable to substitutions at three symmetry-related pairs of amino acid residues as follows: Met-α^D1 (which reduces electrostatic repulsion relative to Val-α^A1), Glu-α^D138 (which increases electrostatic attraction relative to Ala-α^A138), and Ala-α^D134

Table 3. Parameter estimates derived from O_2 equilibrium measurements of pheasant HbA and HbD under the two state Monod-Wyman-Changeux (MWC) allosteric model (compare Figure 3). In separate analyses, the number of O_2-binding sites was freely estimated (q = free) or fixed at 4 (q = 4).

isoHb	°C	pH	IHP/Hb$_4$	P_{50}	n_{50}	n_{max}	P_m	K_T	K_R	L	ΔG	q
				torr			*torr*	*torr^{-1} (± S.E.)*	*torr^{-1} (± S.E.)*		*kJ mol^{-1}*	
HbA												
q = free	25	7.487		4.13	2.60	2.63	3.89	0.0663 ± 0.0054	2.0777 ± 0.3396	1.3×10^4	8.38	4.54
	25	7.050		7.12	2.61	2.65	6.73	0.0316 ± 0.0008	2.1798 ± 0.1974	3.5×10^4	10.10	3.89
fixed q = 4	25	7.487		4.12	2.44	2.47	3.9	0.0637 ± 0.0046	2.4835 ± 0.3419	8.8×10^3	8.74	4.00
	25	7.050		7.13	2.64	2.68	6.73	0.0320 ± 0.0007	2.0496 ± 0.1014	3.6×10^4	9.99	4.00
HbD												
q = free	25	7.492		3.51	2.47	2.49	3.36	0.0752 ± 0.0042	2.0168 ± 0.1706	4.2×10^3	7.99	4.36
	25	7.496	23.5	26.14	2.71	3.02	22.05	0.0162 ± 0.0008	1.2308 ± 0.8497	7.5×10^7	10.20	5.49
	37	7.433		6.05	2.10	2.12	5.72	0.0575 ± 0.0046	1.0665 ± 0.2236	1.7×10^3	7.070	4.10
fixed q = 4	25	7.492		3.50	2.38	2.39	3.36	0.0721 ± 0.0034	2.1948 ± 0.1497	3.0×10^3	8.20	4.00
	25	7.496	23.5	24.2	2.46	2.61	21.5	0.0143 ± 0.0010	2.7×10^5 ± 3.6×10^{10}	1.1×10^{27}	11.70	4.00
	37	7.433		6.05	2.08	2.10	5.72	0.0572 ± 0.0037	1.1053 ± 0.1196	1.6×10^3	7.12	4.00

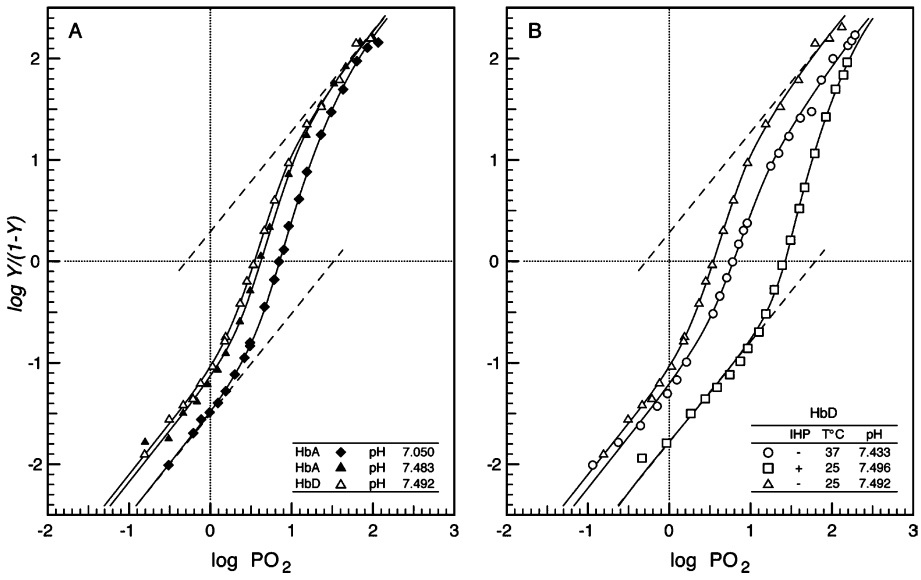

Figure 3. Extended Hill plots of O_2 equilibria (where Y = fractional O_2 saturation) for pheasant HbA and HbD. *A*, HbA and HbD at 25 °C; *B*, HbD at 25 and 37 °C and in the absence and presence of saturating IHP concentration (IHP/Hb ratio = 23.5). In each plot, the intercept of the lower asymptote with the *horizontal line* at log$Y/(Y - 1) = 0$ provides an estimate of K_T, the O_2 association constant of T-state deoxy-Hb, and the intercept of the upper asymptote with the same line provides an estimate of K_R, the O_2 association constant of R-state oxyHb. Heme concentration 0.60 (HbA and HbD); other conditions are as described in the legend for Figure 2.

(which, relative to Thr-α^A134, reduces steric hindrance in the cleft between the α_1 and α_2 subunits).

Discussion

IsoHb Composition of Avian Red Cells. In contrast to the variable patterns of Hb heterogeneity in fishes and other ectothermic vertebrate groups (5, 7–9, 71–73), the two-component HbA/HbD system of birds is remarkably consistent. A number of bird species are known to express three or four structurally distinct isoHbs in definitive erythrocytes (11, 14, 15, 74, 75), but in all such cases HbA and HbD (*i.e.* tetrameric assemblies that incorporate the products of α^A- and α^D-globin, respectively) represent the two main isoforms. HbD expression has also been secondarily lost in a number of avian taxa (*e.g.* pigeons, parakeets, cuckoos, jays, herons, storks, and penguins (74, 76–80)). The same appears to be true for crocodilians (30–32), the sister group to Aves.

Structural and Functional Differentiation between HbA and HbD. It is difficult to pinpoint specific substitutions that may be responsible for isoHb differences in intrinsic O_2 affinity, although substitutions at intersubunit contact surfaces are good candidates: three of the CBD sites (114, 115, and 117) represent $\alpha_1\beta_1$ "packing" contacts. It is also possible that isoHb differences in intrinsic O_2 affinity are attributable to different combinations of substitutions in different species. Studies of isoHb differentiation in the tufted duck, common swift, Rüppell's griffon, and goshawk suggested that the higher O_2 affinity of HbD may be attributable to the possession of Gln-α^D38 or Thr instead of Pro-α^A38 (11, 14, 20, 81–83). In Hbs with αGln-38 or Thr, the R-state (oxy) structure is stabilized by two hydrogen bonds with βHis-97 and βAsp-99, whereas only the latter hydrogen bond is possible in the T-state. Thus, HbD with Gln-α^D38 or Thr is more highly stabilized in the R-state, and the allosteric equilibrium is shifted in favor of this high affinity quaternary structure. This structural mechanism may

contribute to O_2 affinity differences between HbA and HbD in the particular species mentioned above, but it does not provide a general explanation for the observed patterns of functional differentiation between avian HbA and HbD because the majority of bird species retain the ancestral Gln residue at this intersubunit contact site in both α^A- and α^D-globin.

In addition to the isoHb differences in intrinsic O_2 affinity, HbD also exhibits a consistently higher O_2 affinity in the presence of IHP (Tables 1 and 2). This indicates that HbD is less responsive to the inhibitory effects of IHP, a potent allosteric effector that preferentially binds and stabilizes the low affinity T-state quaternary structure of the Hb tetramer. The uniform difference in IHP sensitivity between HbA and HbD is surprising because the main polyphosphate-binding site is formed by a cluster of positively charged β-chain residues that line the interior of the central cavity (18, 84). Because HbA and HbD share identical β-chain subunits (and thus share the same phosphate-binding sites), the observed isoform differences in IHP sensitivity must be attributable to one or more substitutions between α^A- and α^D-globin that do not directly affect the main phosphate-binding site. Experimental evidence suggests that an additional polyphosphate-binding site is formed by seven residues from each α-chain (sites 1, 95, 99, 134, 137, 138, and 141), which stabilize IHP via charge-charge interactions (18, 85, 86). Specifically, αLys-99 and charged residues at the α-chain N and C termini of avian HbA and HbD are predicted to form six salt bridges with the negatively charged phosphate groups of IHP (18, 53). This additional phosphate-binding site is hypothesized to serve as an "entry/leaving site," which modulates Hb-O_2 affinity by enhancing phosphate uptake and transfer to the main oxygenation-linked binding site between the β-chain subunits (18, 53). Of the seven α-chain residues that compose this additional phosphate-binding site, four represent CBD sites that distinguish avian α^A- and α^D-globin sequences (1, 134, 137, and 138). The role of αVal-1 in this additional phosphate-binding site is implicated by the fact that carbamylation of the α-chain N termini produces a 40% reduction in IHP affinity (85). However, even though HbD exhibits a consistently higher O_2 affinity than HbA in the presence of IHP (Tables 1 & 2), our molecular dynamics simulations predict that the additional phosphate-binding site of HbD actually has a slightly lower IHP binding energy (and hence, higher IHP affinity) than that of HbA (Table 4). An alternative hypothesis suggested by results of the molecular dynamics simulations (Figure 6) is that IHP binding between the α_1 and α_2 subunits of HbD produces a second-order perturbation of quaternary structure that is propagated to the main phosphate-binding site between the β-chain subunits.

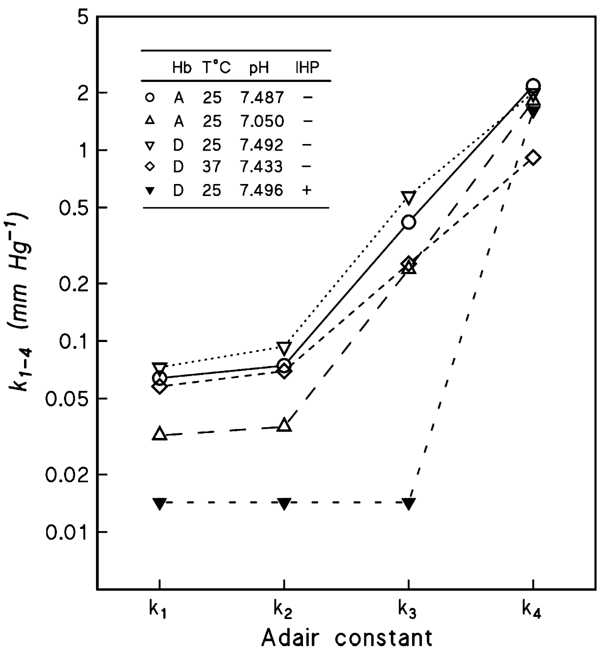

Figure 4. Adair constants (k_1, k_2, k_3, and k_4) for pheasant HbA and HbD as a function of temperature, pH, and the absence and presence of IHP (derived from data shown in Figure 2).

Deoxygenation-linked Self-association of HbD. Our measures of Hb-O_2 equilibria were conducted under standard conditions ([heme] = 0.3 mm (50)) where intrinsic functional differences between tetrameric HbA and HbD were not obscured by possible effects of deoxygenation-linked self-association. Measurements of oxygenation properties under these conditions moreover permit meaningful comparisons with data from previously published studies (Tables 1 and 2). The Hb concentrations used in our experiments greatly exceeded the threshold at which tetrameric vertebrate Hbs dissociate to dimers and monomers (87) but were below the threshold at which deoxygenation-linked self-association of HbD is expected to occur. Thus, our experimental data do not shed light on the prevalence or physiological relevance of HbD self-association in avian red cells. However, available protein expression

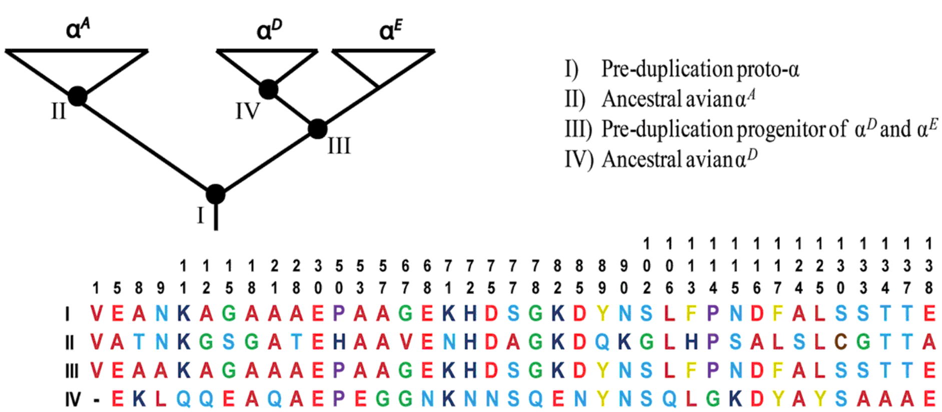

Figure 5. Reconstructed ancestral states of 39 sites that distinguish the α^A- and α^D-globin polypeptides. As shown in the *inset* phylogeny of α-like globin genes, ancestral states for each of the 39 sites were reconstructed for four separate nodes in the tree.

Table 4. Predicted IHP binding affinities for the α- and β-chain polyphosphate-binding sites in homology-based models of pheasant HbA and HbD

IsoHb	IHP-binding site	IHP-binding energy (kcal/mol)
HbA	α-Chain[a]	−5.1
	β-Chain[b]	−6.1
HbD	α-Chain[a]	−6.6
	β-Chain[b]	−6.2

a. The additional polyphosphate-binding site is formed by seven charged residues at or near the N and C termini of the α-chain subunits (sites 1, 95, 99, 134, 137, 138, and 141; Tamburrini *et al.* (18)).
b. The main polyphosphate-binding site is formed by seven charged residues at or near the N and C termini of the β-chain subunits (sites 1, 2, 82, 135, 136, 139, and 143; Tamburrini *et al.* (18)).

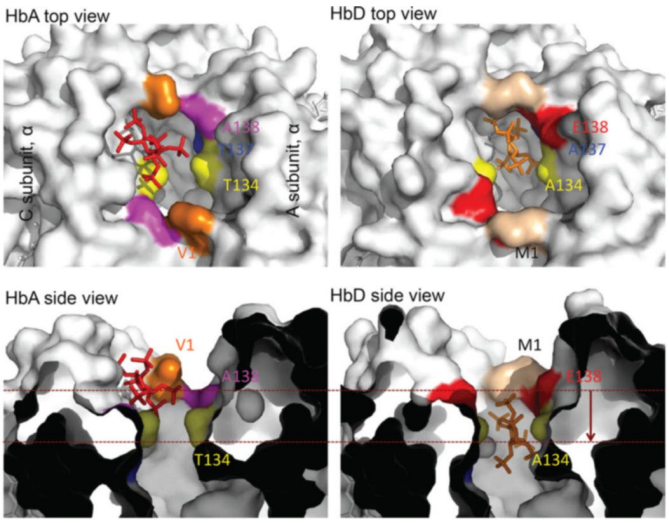

Figure 6. Homology-based structural models of pheasant HbA and HbD showing predicted differences in the stereochemistry of IHP binding between the N and C termini of the α-chain subunits.

data (74, 76–80) indicate that HbD "supercooperativity" in definitive erythrocytes would not be relevant in a number of avian taxa for the simple reason that they do not express HbD during postnatal life.

Our sequence data have implications for long standing questions about the specific residue(s) that mediate the inter-tetramer interactions between deoxy-HbDs (22–24). Because avian HbA and HbD share a common β-chain, interactions between deoxy-HbD tetramers must be mediated by surface residues on the α^D-chain subunit that are not shared with the α^A-chain. On the basis of a crystallographic analysis of chicken R-state HbD, Knapp *et al.* (23) identified four solvent-exposed α^D-chain residues (Met-1, Leu-48, Tyr-89, and Leu-91) that could potentially contribute to the formation of a deoxy-HbD tetramer-tetramer interface. Our comparative analysis of avian α^A- and α^D-globin sequences reveals that only two of these four α-chain residues (1 and 89) are CBD sites (Figure 5). These results demonstrate that phylogenetic surveys of sequence variation can help guide the design of experiments to characterize the structural basis of deoxygenation-linked self-association. Our analysis of sequence conservation in a diverse array of avian taxa helps narrow down the search for causative residues by eliminating sites that do not represent uniformly fixed differences between α^A- and α^D-globin.

Evolutionary Origins of IsoHb Differentiation in Birds. Of the many amino acid substitutions that distinguish avian HbA and HbD, ancestral sequence reconstructions indicate that roughly equal numbers of amino acid substitutions occurred on the post-duplication branches leading to α^A- and α^D-globin. Model-based calculations of electrostatic surface potentials revealed the specific substitutions that are responsible for observed differences in net surface charge between the two isoHbs, and again, roughly equal numbers of these substitutions occurred on the post-duplication branches leading to α^A- and α^D-globin. These results indicate that the observed functional differences between the HbA and HbD isoforms are not attributable to the retention of an ancestral character state from the single-copy, pre-duplication ancestor of the α^E- and α^D-globin genes. The fact that the α^A- and α^D-globin genes have been jointly retained in the majority of sauropsid lineages over the past ~400 million years suggests that the functionally distinct HbA and HbD isoforms have evolved an important physiological division of labor in blood-O_2 transport. The O_2 affinity of HbA is more strongly modulated by allosteric effectors, suggesting that this isoform could play a more important role in modulating blood-O_2 affinity in response to transient changes in O_2 supply or demand, whereas the high affinity HbD may make a more important contribution to blood-O_2 transport under conditions of arterial hypoxemia.

Acknowledgments — We thank Anny Bang (Aarhus, Denmark) and Kathy Williams (Lincoln, NE) for valuable assistance in the laboratory. We also thank Z. A. Cheviron, F. G. Hoffmann, and S. D. Smith for helpful discussions; A. Abbasi and T. Kirkegaard for sharing unpublished data, and two anonymous reviewers for comments and suggestions. We gratefully acknowledge loans from frozen tissue collections at the Museum of Southwestern Biology, the Louisiana Museum of Natural History, and the Florida Museum of Natural History, and we thank M. Berenbrink (University of Liverpool) and C. Witt (University of New Mexico) for sending blood samples.

References

1. Dickerson, R. E., and Geis, I. (1983) *Hemoglobin: Structure, Function, Evolution, and Pathology,* Benjamin/Cummings Publishing, Menlo Park, CA
2. Perutz, M. F. (1983) Species adaptation in a protein molecule. *Mol. Biol. Evol.* 1, 1–28
3. Bunn, H. F., and Forget, B. G. (1986) *Hemoglobin: Molecular, Genetic, and Clinical Aspects,* W.B. Saunders Co., Philadelphia
4. Weber, R. E., and Fago, A. (2004) Functional adaptation and its molecular basis in vertebrate hemoglobins, neuroglobins, and cytoglobins. *Respir. Physiol. Neurobiol.* 144, 141–159
5. Weber, R. E. (1990) in *Animal Nutrition and Transport Processes* (Truchot, J. P., and Lahlou, B., eds) pp. 58–75, S. Karger AG, Basel, Switzerland
6. Weber, R. E. (1995) in *Hypoxia and the Brain: Proceedings of the 9th International Hypoxia Symposium* (Sutton, J. R., Houston, C. S., and Coates, G., eds) pp. 31–44, Queen City Printers, Burlington, VT
7. Weber, R. E. (2000) in *Hemoglobin Function in Vertebrates: Molecular Adaptation in Extreme and Temperate Environments* (Di Prisco, G., Giardina, B., and Weber, R. E., eds) pp. 23–37, Springer-Verlag, Inc., New York
8. Ingermann, R. I. (1997) *Handbook of Physiology,* pp. 357–408, American Physiological Society, Bethesda
9. Weber, R. E., Fago, A., Val, A. L., Bang, A., Van Hauwaert, M. L., Dewilde, S., Zal, F., and Moens, L. (2000) Isohemoglobin differentiation in the bimodal- breathing Amazon catfish *Hoplosternum littorale. J. Biol. Chem.* 275, 17297–17305
10. Baumann, R., Fischer, J., and Engelke, M. (1987) Functional proper-

ties of primitive and definitive red cells from chick embryo. Oxygen-binding characteristics, pH, and membrane potential and response to hypoxia. *J. Exp. Zool. Suppl.* 1, 227–238
11. Hiebl, I., Weber, R. E., Schneeganss, D., Kösters, J., and Braunitzer, G. (1988) High altitude respiration of birds. Structural adaptations in the major and minor hemoglobin component of adult Rüppell's griffon (*Gyps rueppellii*, Aegypiinae). A new molecular pattern for hypoxic tolerance. *Biol. Chem. Hoppe-Seyler* 369, 217–232
12. Hiebl, I., Weber, R. E., Schneeganss, D., and Braunitzer, G. (1989) High altitude respiration of Falconiformes. The primary structure and functional properties of the major and minor hemoglobin components of the adult white-headed vulture (*Trigonoceps occipitalis*, Aegypiinae). *Biol. Chem. Hoppe-Seyler* 370, 699–706
13. Isaacks, R. E., Harkness, D. R., Adler, J. L., and Goldman, P. H. (1976) Studies on avian erythrocyte metabolism. Effect of organic phosphates on oxygen affinity of embryonic and adult-type hemoglobins of the chick embryo. *Arch. Biochem. Biophys.* 173, 114–120
14. Nothum, R., Weber, R. E., Kösters, J., Schneeganss, D., and Braunitzer, G. (1989) Amino acid sequences and functional differentiation of hemoglobins A and D from swift (*Apus*, Apodiformes). *Biol. Chem. Hoppe-Seyler* 370, 1197–1207
15. Oberthür, W., Braunitzer, G., Baumann, R., and Wright, P. G. (1983) Primary structures of the _- and _-chains from the major hemoglobin component of the ostrich (*Struthio camelus*) and American rhea (*Rhea americana*) (Struthioformes). Aspects of respiratory physiology and taxonomy. *Hoppe-Seyler's Z. Physiol. Chem.* 363, 119–134
16. Rana, M. S., Knapp, J. E., Holland, R. A., and Riggs, A. F. (2008) Component D of chicken hemoglobin and the hemoglobin of the embryonic Tammar wallaby (*Macropus eugenii*) self-associate upon deoxygenation. Effect on oxygen binding. *Proteins* 70, 553–561
17. Sanna, M. T., Manconi, B., Podda, G., Olianas, A., Pellegrini, M., Castagnola, M., Messana, I., and Giardina, B. (2007) Alkaline Bohr effect of bird hemoglobins. The case of the flamingo. *Biol. Chem.* 388, 787–795
18. Tamburrini, M., Riccio, A., Romano, M., Giardina, B., and di Prisco, G. (2000) Structural and functional analysis of the two hemoglobins of the Antarctic seabird *Catharacta maccormicki*. Characterization of an additional phosphate-binding site by molecular modeling. *Eur. J. Biochem.* 267, 6089–6098
19. Vandecasserie, C., Paul, C., Schnek, A. G., and Le´onis, J. (1973) Oxygen affinity of avian hemoglobins. *Comp. Biochem. Physiol. A* 44, 711–718
20. Weber, R. E., Hiebl, I., and Braunitzer, G. (1988) High altitude and hemoglobin function in the vultures *Gyps rueppellii* and *Aegypius* monachus. *Biol. Chem. Hoppe-Seyler* 369, 233–240
21. Lutz, P. L. (1980) On the oxygen affinity of bird blood. *Am. Zool.* 20, 187–198
22. Cobb, J. A., Manning, D., Kolatkar, P. R., Cox, D. J., and Riggs, A. F. (1992) Deoxygenation-linked association of a tetrameric component of chicken hemoglobin. *J. Biol. Chem.* 267, 1183–1189
23. Knapp, J. E., Oliveira, M. A., Xie, Q., Ernst, S. R., Riggs, A. F., and Hackert, M. L. (1999) The structural and functional analysis of the hemoglobin D component from chicken. *J. Biol. Chem.* 274, 6411–6420
24. Rana, M. S., and Riggs, A. F. (2011) Indefinite noncooperative self-association of chicken deoxy hemoglobin D. *Proteins* 79, 1499–1512
25. Riggs, A. F. (1998) Self-association, cooperativity, and supercooperativity of oxygen binding by hemoglobins. *J. Exp. Biol.* 201, 1073–1084
26. Perutz, M. F., Steinkraus, L. K., Stockell, A., and Bangham, A. D. (1959) Chemical and crystallographic study of the two fractions of adult horse hemoglobin. *J. Mol. Biol.* 1, 402–404
27. Riggs, A. (1976) Factors in the evolution of hemoglobin function. *Fed. Proc.* 35, 2115–2118
28. Riggs, A. (1979) Studies of the hemoglobins of Amazonian fishes. Overview. *Comp. Biochem. Physiol.* 62, 257–272
29. Nikinmaa, M. (2001) Hemoglobin function in vertebrates. Evolutionary changes in cellular regulation in hypoxia. *Respir. Physiol.* 128, 317–329
30. Jensen, F. B. (2004) Red blood cell pH, the Bohr effect, and other oxygenation- linked phenomena in blood O2 and CO2 transport. *Acta Physiol. Scand.* 182, 215–227
31. Hoffmann, F. G., and Storz, J. F. (2007) The _*D*-globin gene originated via duplication of an embryonic_-like globin gene in the ancestor of tetrapod vertebrates. *Mol. Biol. Evol.* 24, 1982–1990
32. Hoffmann, F. G., Storz, J. F., Gorr, T. A., and Opazo, J. C. (2010) Lineagespecific patterns of functional diversification in the α- and β-globin gene families of tetrapod vertebrates. *Mol. Biol. Evol.* 27, 1126–1138
33. Storz, J. F., Opazo, J. C., and Hoffmann, F. G. (2011) Phylogenetic diversification of the globin gene superfamily in chordates. *IUBMB Life* 63, 313–322
34. Cirotto, C., Panara, F., and Arangi, I. (1987) The minor hemoglobins of primitive and definitive erythrocytes of the chicken embryo. Evidence for hemoglobin L. *Development* 101, 805–813
35. Alev, C., Shinmyozu, K., McIntyre, B. A., and Sheng, G. (2009) Genomic organization of zebra finch α- and β-globin genes and their expression in primitive and definitive blood in comparison with globins in chicken. *Dev. Genes Evol.* 219, 353–360
36. Storz, J. F., Hoffmann, F. G., Opazo, J. C., Sanger, T. J., and Moriyama, H. (2011) Developmental regulation of hemoglobin synthesis in the green anole lizard, *Anolis carolinensis*. *J. Exp. Biol.* 214, 575–581
37. Weber, R. E., and White, F. N. (1986) Oxygen binding in alligator blood related to temperature, diving, and "alkaline tide." *Am. J. Physiol.* 251, R901–R908
38. Weber, R., and White, F. (1994) Chloride-dependent organic phosphate sensitivity of the oxygenation reaction in crocodilian hemoglobins. *J. Exp. Biol.* 192, 1–11
39. Grigg, G. C., Wells, R. M. G., and Beard, L. A. (1993) Allosteric control of oxygen binding by hemoglobin during development in the crocodile *Crocodylus porosus*. The role of red cell organic phosphates and carbon dioxide. *J. Exp. Biol.* 175, 15–32
40. Hoffmann, F. G., Opazo, J. C., and Storz, J. F. (2008) Rapid rates of lineagespecific gene duplication and deletion in the α-globin gene family. *Mol. Biol. Evol.* 25, 591–602
41. Hoffmann, F. G., Opazo, J. C., and Storz, J. F. (2011) Differential loss and retention of myoglobin, cytoglobin, and globin-E during the radiation of vertebrates. *Genome Biol. Evol.* 3, 588–600
42. Brittain, T. (2002) Molecular aspects of embryonic hemoglobin function. *Mol. Aspects Med.* 23, 293–342
43. Weber, R. E., Ostojic, H., Fago, A., Dewilde, S., Van Hauwaert, M. L., Moens, L., and Monge, C. (2002) Novel mechanism for high altitude adaptation in hemoglobin of the Andean frog *Telmatobius peruvianus*. *Am. J. Physiol. Regul. Integr. Comp. Physiol.* 283, R1052–R1060
44. Weber, R. E., Voelter, W., Fago, A., Echner, H., Campanella, E., and Low, P. S. (2004) Modulation of red cell glycolysis. Interactions between vertebrate hemoglobins and cytoplasmic domains of band 3 red cell membrane proteins. *Am. J. Physiol. Regul. Integr. Comp. Physiol.* 287, R454–R464
45. Brygier, J., and Paul, C. (1976) Oxygen equilibrium of chicken hemoglobin in the presence of organic phosphates. *Biochimie* 58, 755–756
46. Monod, J., Wyman, J., and Changeux, J. P. (1965) On the nature of allosteric transitions. A plausible model. *J. Mol. Biol.* 12, 88–118
47. Weber, R. E., Malte, H., Braswell, E. H., Oliver, R. W., Green, B. N., Sharma, P. K., Kuchumov, A., and Vinogradov, S. N. (1995) Mass spectrometric composition, molecular mass, and oxygen binding of *Macrobdella decora* hemoglobin and its tetramer and monomer subunits. *J. Mol. Biol.* 251, 703–720
48. Adair, G. S. (1925) The hemoglobin system. IV. The oxygen dissociation curve of hemoglobin. *J. Biol. Chem.* 63, 529–545
49. Ferry, M. F., and Green, A. A. (1929) Studies in the chemistry of hemoglobin. III. The equilibrium between oxygen and hemoglobin and its relation to changing hydrogen ion activity. *J. Biol. Chem.* 81, 175–203
50. Imai, K. (1982) *Allosteric Effects in Hemoglobin,* Cambridge University, Press, Cambridge, UK

51. Weber, R. E. (1992) Use of ionic and zwitterionic (Tris/BisTris and HEPES) buffers in studies on hemoglobin function. *J. Appl. Physiol.* 72, 1611–1615
52. Arnold, K., Bordoli, L., Kopp, J., and Schwede, T. (2006) The SWISSMODEL Workspace. A web-based environment for protein structure homology modeling. *Bioinformatics* 22, 195–201
53. Riccio, A., Tamburrini, M., Giardina, B., and di Prisco G. (2001) Molecular dynamics analysis of a second phosphate site in the hemoglobins of the seabird, south polar skua. Is there a site-site migratory mechanism along the central cavity? *Biophys. J.* 81, 1938–1946
54. Jo, S., Kim, T., Iyer, V. G., and Im, W. (2008) CHARMM-GUI. A webbased graphical user interface for CHARMM. *J. Comput. Chem.* 29, 1859–1865
55. Gasteiger, E., Gattiker, A., Hoogland, C., Ivanyi, I., Appel, R. D., and Bairoch, A. (2003) ExPASy. The proteomics server for in-depth protein knowledge and analysis. *Nucleic Acids Res.* 31, 3784–3788
56. Trott, O., and Olson, A. J. (2010) AutoDock Vina. Improving the speed and accuracy of docking with a new scoring function, efficient optimization, and multithreading. *J. Comput. Chem.* 31, 455–461
57. Hoffmann, F. G., Opazo, J. C., and Storz, J. F. (2012) Whole-genome duplication spurred the functional diversification of the globin gene superfamily in vertebrates. *Mol. Biol. Evol.* 29, 303–312
58. Gribaldo, S., Casane, D., Lopez, P., and Philippe, H. (2003) Functional divergence prediction from evolutionary analysis. A case study of vertebrate hemoglobin. *Mol. Biol. Evol.* 20, 1754–1759
59. Gu, X. (2001) Maximum-likelihood approach for gene family evolution under functional divergence. *Mol. Biol. Evol.* 18, 453–464
60. Shannon, C. E. (1948) A mathematical theory of communication. *Bell System Tech. J.* 27, 379–423, 623–656
61. Yang, Z., Kumar, S., and Nei, M. (1995) A new method of inference of ancestral nucleotide and amino acid sequences. *Genetics* 141, 1641–1650
62. Cao, Y., Adachi, J., Janke, A., Pa¨a¨bo, S., and Hasegawa, M. (1994) Phylogenetic relationships among eutherian orders estimated from inferred sequences of mitochondrial proteins. Instability of a tree based on a single gene. *J. Mol. Evol.* 39, 519–527
63. Whelan, S., and Goldman, N. (2001) A general empirical model of protein evolution derived from multiple protein families using a maximum-likelihood approach. *Mol. Biol. Evol.* 18, 691–699
64. Yang, Z. (2007) PAML 4. Phylogenetic analysis by maximum likelihood. *Mol. Biol. Evol.* 24, 1586–1591
65. Edgar, R. C. (2004) MUSCLE. Multiple sequence alignment with high accuracy and high throughput. *Nucleic Acids Res.* 32, 1792–1797
66. Hackett, S. J., Kimball, R. T., Reddy, S., Bowie, R. C., Braun, E. L., Braun, M. J., Chojnowski, J. L., Cox, W. A., Han, K. L., Harshman, J., Huddleston, C. J., Marks, B. D., Miglia, K. J., Moore, W. S., Sheldon, F. H., Steadman, D. W., Witt, C. C., and Yuri, T. (2008) A phylogenomic study of birds reveals their evolutionary history. *Science* 320, 1763–1768
67. Gill, S. J., Gaud, H. T., and Barisas, B. G. (1980) Calorimetric studies of carbon monoxide and inositol hexaphosphate binding to hemoglobin A. *J. Biol. Chem.* 255, 7855–7857
68. Wyman, J., Jr. (1964) Linked functions and reciprocal effects in hemoglobin. A second look. *Adv. Protein Chem.* 19, 223–286
69. Tyuma, I., Imai, K., and Shimizu, K. (1973) Analysis of oxygen equilibrium of hemoglobin and control mechanism of organic phosphates. *Biochemistry* 12, 1491–1498
70. Weber, R. E., Jensen, F. B., and Cox, R. P. (1987) Analysis of teleost hemoglobin by Adair and Monod-Wyman-Changeux models. Effects of nucleoside triphosphates and pH on oxygenation of tench hemoglobin. *J. Comp. Physiol. B* 157, 145–152
71. Binotti, I., Giovenco, S., Giardina, B., Antonini, E., Brunori, M., and Wyman, J. (1971) Studies on the functional properties of fish hemoglobins. II. The oxygen equilibrium of the isolated hemoglobin components from trout blood. *Arch. Biochem. Biophys.* 142, 274–280
72. Weber, R. E., and Jensen, F. B. (1988) Functional adaptations in hemoglobins from ectothermic vertebrates. *Annu. Rev. Physiol.* 50, 161–179
73. Weber, R. E. (1996) in *Physiology and Biochemistry of the Fishes of the Amazon* (Val, A. L., Almeida-Val, V. M., and Randall, D. J., eds) pp. 75–90, INPA, Brazil
74. Saha, A., and Ghosh, J. (1965) Comparative studies on avian hemoglobins. *Comp. Biochem. Physiol.* 15, 217–235
75. Lee, K. S., Huang, P. C., and Cohen, B. H. (1976) Further resolution of adult chick hemoglobins by isoelectric focusing in polyacrylamide gel. *Biochim. Biophys. Acta* 427, 178–196
76. Godovac-Zimmermann, J., and Braunitzer, G. (1984) Hemoglobin of the adult white stork (*Ciconia*, Ciconiiformes). The primary structure of α^A- and β-chains from the only present hemoglobin component. *Hoppe-Seyler's Z. Physiol. Chem.* 365, 1107–1113
77. Godovac-Zimmermann, J., and Braunitzer, G. (1985) The primary structure of α^A- and β-chains from blue-and-yellow macaw (*Ara ararauna*, Psittaci) hemoglobin. No evidence for expression of α^D-chains. *Biol. Chem. Hoppe-Seyler* 366, 503–508
78. Oberthür, W., Godovac-Zimmermann, J., and Braunitzer, G. (1986) The expression of α^D-chains in the hemoglobin of adult ostrich (*Struthio camelus*) and American rhea (*Rhea americana*). The different evolution of adult bird α^A-, α^D-, and β-chains. *Biol. Chem. Hoppe-Seyler* 367, 507–514
79. Sultana, C., Abbasi, A., and Zaidi, Z. H. (1989) Primary structure of hemoglobin α-chain of *Columba livia* (gray wild pigeon). *J. Protein Chem.* 8, 629–646
80. Tamburrini, M., Condò, S. G., di Prisco, G., and Giardina, B. (1994) Adaptation to extreme environments. Structure-function relationships in emperor penguin hemoglobin. *J. Mol. Biol.* 237, 615–621
81. Hiebl, I., Kösters, J., and Braunitzer, G. (1987) The primary structures of the major and minor hemoglobin component of adult goshawk (*Accipiter gentilis,* Accipitrinae). *Biol. Chem. Hoppe-Seyler* 368, 333–342
82. Abbasi, A., and Lutfullah, G. (2002) Molecular basis of bird respiration. Primary hemoglobin structure component from tufted duck (*Aythya fuligula*, Anseriformes). Role of αArg-99 in formation of a complex salt bridge network. *Biochem. Biophys. Res. Commun.* 291, 176–184
83. Lutfullah, G., Ali, S. A., and Abbasi, A. (2005) Molecular mechanism of high altitude respiration. Primary structure of a minor hemoglobin component from tufted duck (*Aythya fuligula*, Anseriformes). *Biochem. Biophys. Res. Commun.* 326, 123–130
84. Arnone, A., and Perutz, M. F. (1974) Structure of inositol hexaphosphatehuman deoxyhemoglobin complex. *Nature* 249, 34–36
85. Zuiderweg, E. R., Hamers, L. F., Rollema, H. S., de Bruin, S. H., and Hilbers, C. W. (1981) 31P NMR study of the kinetics of binding of myo-inositol hexakisphosphate to human hemoglobin. Observation of fast exchange kinetics in high affinity systems. *Eur. J. Biochem.* 118, 95–104
86. Amiconi, G., Bertollini, A., Bellelli, A., Coletta, M., Condò, S. G., and Brunori, M. (1985) Evidence for two oxygen-linked binding sites for polyanions in dromedary hemoglobin. *Eur. J. Biochem.* 150, 387–393
87. Mills, F. C., Johnson, M. L., and Ackers, G. K. (1976) Oxygenation-linked subunit interactions in human hemoglobin. Experimental studies on the concentration dependence of oxygenation curves. *Biochemistry* 15, 5350–5362

Supplementary Tables

Table S1. Accession numbers for avian α-like globin sequences.

Order	Family	Species	Accession number
Accipitriformes	Accipitridae	Northern goshawk, *Accipiter gentilis*	P08850.2, P08849.1
Accipitriformes	Accipitridae	Black vulture, *Aegypius monachus*	P07417.2, P68059.1
Accipitriformes	Accipitridae	Rüppell's griffon, *Gyps rueppellii*	P08256.1, P08257.1
Accipitriformes	Accipitridae	White-headed vulture, *Trigonoceps occipitalis*	P19832.1, P68060.1
Anseriformes	Anatidae	Mallard duck, *Anas platyrhynchos*	P01988.2, P04442.1, K01942.1
Anseriformes	Anatidae	Graylag goose, *Anser anser*	P01989.2, P04238.1
Anseriformes	Anatidae	Bar-headed goose, *Anser indicus*	P01990.2, P04239.1
Anseriformes	Anatidae	Tufted duck, *Aythya fuligula*	P84790.2, P84791.1
Anseriformes	Anatidae	Canada goose, *Branta canadensis*	ACT80863.1, P04240.1
Anseriformes	Anatidae	Muscovy duck, *Cairina moschata*	P01987.2, P02003.1, P04243.2
Anseriformes	Anatidae	Andean goose, *Chloephaga melanoptera*	ACT80387.1, P07035.1
Apodiformes	Apodidae	Common swift, *Apus apus*	P15162.2, P15164.1
Apodiformes	Trochilidae	Speckled hummingbird, *Adelomyia melanogenys*	JQ697045, JQ697061
Apodiformes	Trochilidae	White-tufted sunbeam, *Aglaeactis castelnaudii*	JQ697046, JQ697062
Apodiformes	Trochilidae	Amazilia hummingbird, *Amazilia amazilia*	JQ697047, JQ697063
Apodiformes	Trochilidae	Green-and-white hummingbird, *Amazilia viridicauda*	JQ697048, JQ697064
Apodiformes	Trochilidae	Bronzy inca, *Coeligena coeligena*	JQ697049, JQ697065
Apodiformes	Trochilidae	Violet-throated starfrontlet, *Coeligena violifer*	JQ697050, JQ697066
Apodiformes	Trochilidae	Andean hillstar, *Oreotrochilus estella*	JQ697051, JQ405318
Apodiformes	Trochilidae	Black-breasted hillstar, *Oreotrochilus melanogaster*	JQ697052, JQ697067
Apodiformes	Trochilidae	Giant hummingbird, *Patagona gigas*	JQ697054, JQ697060
Apodiformes	Trochilidae	Great-billed hermit, *Phaethornis malaris*	JQ697053 , JQ697059
Charadriiformes	Stercorariidae	South polar skua, *Catharacta maccormicki*	P82111.1, P82112.1
Columbiformes	Columbidae	Rock pigeon, *Columba livia*	P21871.2, O12985.1, JQ405311
Cuculiformes	Cuculidae	Common cuckoo, *Cuculus canorus*	BAC57968, BAC57969.1
Falconiformes	Falconidae	Prairie falcon, *Falco mexicanus*	JQ405314
Galliformes	Phasianidae	Japanese quail, *Coturnix japonica*	P24589.2, P30892.1
Galliformes	Phasianidae	Chicken, *Gallus gallus*	NP_001004376, NP_001004375.1, NP_001004374.1
Galliformes	Phasianidae	Wild turkey, *Meleagris gallopavo*	P81023.2, P81024.1, XP_003210789.1
Galliformes	Phasianidae	Common pheasant, *Phasianus colchicus*	P01995.1, P02002.1
Gruiformes	Gruidae	Sandhill crane, *Grus canadensis*	JQ405312
Opisthocomiformes	Opisthocomidae	Hoatzin, *Opisthocomus hoazin*	JQ405310
Passeriformes	Corvidae	Hooded crow, *Corvus cornix*	JQ697055, JQ405319
Passeriformes	Emberizidae	Rufous-collared sparrow, *Zonotrichia capensis*	JQ405316, JQ405315
Passeriformes	Estrildidae	Zebra finch, *Taeniopygia guttata*	XP_002196132.1, XP_002196147.1, NP_001191174.1
Passeriformes	Furnariidae	Wren-like rushbird, *Phleocryptes melanops*	JQ405307, JQ405317
Passeriformes	Passeridae	Tree sparrow, *Passer montanus*	P07407.1, P07413.1, JQ405308
Passeriformes	Sturnidae	Yellow-faced myna, *Mino dumontii*	JQ697056, JQ697069
Passeriformes	Sturnidae	Common starling, *Sturnus vulgaris*	P01997.1, P02004.1, JQ405313
Passeriformes	Troglodytidae	House wren, *Troglodytes aedon*	JQ405324, JQ697068
Passeriformes	Turdidae	Common blackbird, *Turdus merula*	P14522.1, P14523.1
Pelecaniformes	Pelecanidae	Dalmatian pelican, *Pelecanus crispus*	JQ405326, JQ405322
Pelecaniformes	Pelecanidae	Great white pelican, *Pelecanus onocrotalus*	JQ405325, JQ824132
Pelecaniformes	Phalacrocoracidae	Great cormorant, *Phalacrocorax carbo*	P10780.1, P10781.1, JQ405309
Phoenicopteriformes	Phoenicopteridae	Greater flamingo, *Phoenicopterus roseus*	JQ697057, JQ697070
Phoenicopteriformes	Phoenicopteridae	American flamingo, *Phoenicopterus ruber*	P01984.2, JQ405321
Psittaciformes	Psittacidae	Budgerigar, *Melopsittacus undulatus*	JQ697058
Psittaciformes	Psittacidae	Rose-ringed parakeet, *Psittacula krameri*	P19831.1
Strigiformes	Strigidae	Eurasian eagle owl, *Bubo bubo*	JQ405323, JQ405320
Struthioniformes	Rheidae	Greater rhea, *Rhea americana*	P01982.1, P04241.1
Struthioformes	Struthionidae	Ostrich, *Struthio camelus*	P01981.1, P04242.1

Table S2. Accession numbers for α-like globin sequences from nonavian vertebrates.

Class	Order	Family	Species	Accession number
Actinopterygii	Beloniformes	Adrianichthyidae	Japanese medaka, *Oryzias latipes*	BAC20295.1, BAC06482.1
Actinopterygii	Characiformes	Characidae	Red-tailed brycon, *Brycon cephalus*	ABL89191.1
Actinopterygii	Cypriniformes	Cyprinidae	Common carp, *Cyprinus carpio*	BAB79237.1
Actinopterygii	Cypriniformes	Cyprinidae	Zebrafish, *Danio rerio*	NP_891985.1
Actinopterygii	Esociformes	Esocidae	Northern pike, *Esox lucius*	ACO13595.1
Actinopterygii	Gadiformes	Gadidae	Polar cod, *Boreogadus saida*	Q1AGS9.3
Actinopterygii	Gadiformes	Gadidae	Atlantic cod, *Gadus morhua*	ABV21551.1
Actinopterygii	Osmeriformes	Osmeridae	Rainbow smelt, *Osmerus mordax*	ACO08865.1
Actinopterygii	Perciformes	Osmeridae	Antartic fish, *Pogonophryne scotti*	P0C238.2
Actinopterygii	Perciformes	Osmeridae	Yellow perch, *Perca flavescens*	1XQ5_A
Actinopterygii	Pleuronectiformes	Osmeridae	Turbot, *Scophthalmus maximus*	ABJ98630.1
Actinopterygii	Salmoniformes	Osmeridae	Rainbow trout, *Oncorhynchus mykiss*	ACO08763.1
Actinopterygii	Salmoniformes	Osmeridae	Atlantic salmon, *Salmo salar*	CAA65949.1
Actinopterygii	Scorpaeniformes	Osmeridae	Sablefish, *Anoplopoma fimbria*	ACQ58238.1
Actinopterygii	Scorpaeniformes	Osmeridae	Kelp snailfish, *Liparis tunicatus*	P85081.1
Actinopterygii	Siluriformes	Osmeridae	Channel catfish, *Ictalurus punctatus*	NP_001188201.1
Actinopterygii	Tetraodontiformes	Osmeridae	Fugu rubripes, *Takifugu rubripes*	AAO61492.1
Actinopterygii	Tetraodontiformes	Osmeridae	Pufferfish, *Tetraodon nigroviridis*	CAG12202.1
Amphibia	Anura	Pipidae	African clawed frog, *Xenopus laevis*	P02012.2, NP_001081493.1, P06636.2, NP_001079749.1, NP_001079746.1
Amphibia	Anura	Pipidae	Western clawed frog, *Xenopus tropicalis*	NP_988860.1, NP_001005092.1, NP_001135724.1, NP_001165373.1, NP_001107321.1, NP_001165374.1, NP_001015904.1, NP_001016009.1
Amphibia	Anura	Ranidae	Bullfrog, *Rana catesbeiana*	P51465.2, ACO51559.1, P55267.2
Amphibia	Caudata	Ambystomatidae	Axolotl, *Ambystoma mexicanum*	P02015.2, AAK58843.1, BAD30048.1, BAD30049.1
Amphibia	Caudata	Salamandridae	Iberian ribbed newt, *Pleurodeles waltl*	P06639.4, P11896.1
Amphibia	Caudata	Salamandridae	Rough-skinned newt, *Taricha granulosa*	P02014.1, P10783.1
Mammalia	Carnivora	Canidae	Dog, *Canis lupus*	P60529.1
Mammalia	Carnivora	Felidae	Domestic cat, *Felis catus*	P07405.1
Mammalia	Carnivora	Ursidae	Giant panda, *Ailuropoda melanoleuca*	XP_002920201.1, XP_002920198.1
Mammalia	Cetacea	Delphinidae	Saddleback dolphin, *Delphinus delphis*	ACN44165.1
Mammalia	Cetacea	Delphinidae	Bottlenosed dolphin, *Tursiops truncatus*	P18978.1
Mammalia	Cetacea	Physeteridae	Sperm whale, *Physeter catodon*	P09904.1
Mammalia	Cetartiodactyla	Bovidae	Cattle, *Bos taurus*	NP_001070890.2, XP_001788743.1, XP_580707.3
Mammalia	Cetartiodactyla	Bovidae	Goat, *Capra hircus*	ACH86006.1, P13786.2
Mammalia	Cetartiodactyla	Suidae	Pig, *Sus scrofa*	XP_003481132.1, P02009.1
Mammalia	Chiroptera	Molossidae	Wrinkle-lipped free-tailed bat, *Chaerephon plicatus*	ACE60603.1
Mammalia	Chiroptera	Pteropodidae	Leschenault's rousette, *Rousettus leschenaultii*	ACE60609.1
Mammalia	Chiroptera	Phyllostomidae	California leaf-nosed bat, *Macrotus californicus*	P09839.1
Mammalia	Cingulata	Dasypodidae	Nine-banded armadillo, *Dasypus novemcinctus*	P01964.1, ACO83100.1
Mammalia	Didelphimorphia	Didelphidae	Gray short-tailed opossum, *Monodelphis domestica*	NP_001028158.1, XP_003341721.1
Mammalia	Diprotodontia	Macropodidae	Tammar wallaby, *Macropus eugenii*	P81043.3, AAX18654.1, AAX18653.1
Mammalia	Insectivora	Erinaceidae	Western European hedgehog, *Erinaceus europaeus*	P01949.1
Mammalia	Insectivora	Soricidae	European shrew, *Sorex araneus*	ACE73634.1, ACE73631.1
Mammalia	Insectivora	Talpidae	Coast mole, *Scapanus orarius*	ADJ17347.1
Mammalia	Insectivora	Talpidae	European mole, *Talpa europaea*	P01951.1
Mammalia	Lagomorpha	Leporidae	European hare, *Lepus europaeus*	3LQD_A
Mammalia	Lagomorpha	Leporidae	Rabbit, *Oryctolagus cuniculus*	NP_001075858.1, NP_001164886.1
Mammalia	Lagomorpha	Ochotonidae	Black-lipped pika, *Ochotona curzoniae*	ABO27190.1
Mammalia	Monotremata	Ornithorhynchidae	Platypus, *Ornithorhynchus anatinus*	XP_001517140.2, XP_001510395.1
Mammalia	Perissodactyla	Equidae	Horse, *Equus caballus*	P01958.2, NP_001108014.1
Mammalia	Perissodactyla	Rhinocerotidae	White rhinoceros, *Ceratotherium simum*	P01963.2

Table S2. Accession numbers for α-like globin sequences from nonavian vertebrates *(continued)*.

Class	Order	Family	Species	Accession number
Mammalia	Perissodactyla	Tapiridae	Brazilian tapir, *Tapirus terrestris*	P01962.1
Mammalia	Primates	Hominidae	Human, *Homo sapiens*	NP_000508.1, NP_005323.1
Mammalia	Primates	Atelidae	Black-handed spider monkey, *Ateles geoffroyi*	P67817.2
Mammalia	Primates	Cebidae	White-tufted-ear marmoset, *Callithrix jacchus*	XP_002755769.1, ABZ80335.1
Mammalia	Proboscidea	Elephantidae	Asiatic elephant, *Elephas maximus*	ACV41393.1
Mammalia	Proboscidea	Elephantidae	African savanna elephant, *Loxodonta africana*	XP_003417852.1, XP_003417854.1
Mammalia	Rodentia	Cricetidae	Chinese hamster, *Cricetulus griseus*	XP_003501524.1, XP_003511891.1
Mammalia	Rodentia	Cricetidae	Deer mouse, *Peromyscus maniculatus*	ABN71059.1, ABN71228.1
Mammalia	Rodentia	Muridae	Norway rat, *Rattus norvegicus*	NP_001013875.1, NP_001166316.1
Reptilia	Crocodylia	Crocodylidae	Nile crocodile, *Crocodylus niloticus*	P01998.1
Reptilia	Crocodylia	Crocodylidae	American alligator, *Alligator mississippiensis*	P01999.2
Reptilia	Crocodylia	Crocodylidae	Spectacled caiman, *Caiman crocodilus*	0901255A, P02000.1
Reptilia	Sphenodontia	Sphenodontidae	Tuatara, *Sphenodon punctatus*	P10059.1, P10062.1
Reptilia	Squamata	Colubridae	Texas indigo snake, *Drymarchon corais*	P0C0U6.1, P0C0U7.1
Reptilia	Squamata	Iguanidae	Marine iguana, *Amblyrhynchus cristatus*	Gorr (1)
Reptilia	Squamata	Iguanidae	Green anole, *Anolis carolinensis*	Hoffman *et al.* (2)
Reptilia	Testudines	Cheloniidae	Loggerhead turtle, *Caretta caretta*	Q10732.1
Reptilia	Testudines	Emydidae	Western painted turtle, *Chrysemys picta*	P13273.1, P02005.1
Reptilia	Testudines	Emydidae	Red-eared slider turtle, *Trachemys scripta*	FG341498.1
Reptilia	Testudines	Testudinidae	Brazilian giant tortoise, *Geochelone denticulata*	AAM18964.1
Reptilia	Testudines	Testudinidae	Galápagos giant tortoise, *Geochelone nigra*	P83135.2
Reptilia	Testudines	Chelidae	Snake-necked turtle, *Phrynops hilarii*	P02006.1

References - Supplementary Material

1. Gorr, T. (1993) *Haemoglobine: Sequenz und Phylogenie. Die Primärstruktur von Globinketten des Quastenflossers (Latimeria chalumnae) sowie folgender Reptilien: Galapagos-Meerechse (Amblyrhynchus cristatus), Grüner Leguan (Iguana iguana), Indigonatter (Drymarchon corais), Glattstirnkaiman (Paleosuchus palpebrosus).* Ph.D. Thesis, University of Munich, Germany.

2. Hoffmann, F.G., Storz, J.F., Gorr, T.A., and Opazo, J.C. (2010) Lineage-specific patterns of functional diversification in the α- and β-globin gene families of tetrapod vertebrates. *Mol. Biol. Evol.* **27**, 1126-1138